Formation and local symmetry of the Holstein polaron in the *t–J* model

Han Ma[1]**, T K Lee**[2] **and Yan Chen**[1,3,4]

[1] Department of Physics, State Key Laboratory of Surface Physics and Laboratory of Advanced Materials, Fudan University, Shanghai 200433, People's Republic of China
[2] Institute of Physics, Academia Sinica, NanKang, Taipei 11529, Taiwan
[3] Department of Physics and Center of Theoretical and Computational Physics, The University of Hong Kong, Pokfulam Road, Hong Kong, People's Republic of China
E-mail: yanchen99@fudan.edu.cn

Abstract. The formation and local symmetry of a spin–lattice polaron has been investigated semiclassically in planar Holstein t–J-like models within the exact diagonalization method. Due to the interplay of strong correlations and electron–lattice interaction, the doped hole may either move freely or lead to the localized spin–lattice distortion and form a Holstein polaron. The formation of a polaron breaks the translational symmetry by suppression of antiferromagnetic correlations and inducement of ferromagnetic correlations locally. Moreover, the breaking of local rotational symmetry around the polaron has been shown. The ground state is generically a parity singlet and the first excited state may be a parity doublet. Further consequences of the density of states spectra for comparison with scanning tunneling microscopy experiments are discussed.

Doping a Mott insulator is regarded as the main physics in high T_c cuprate superconductors [1]. A single hole in the two-dimensional t–J model may form a ferromagnetic (FM) spin polaron for sufficiently small exchange coupling J [2]. For finite J, the distortion of the antiferromagnetic (AFM) background decays away from the hole and the competition between

[4] Author to whom any correspondence should be addressed.

magnetic correlation and kinetic energy may result in the ground state with a spin polaron structure. This problem has been extensively investigated numerically [3–7]. To provide a better comparison with angle-resolved photoemission spectroscopy (ARPES) experimental data, one needs to include the nearest-neighboring (NN) and next-nearest-neighboring (NNN) hopping t' and t'' terms [8–10]. On the other hand, the role of electron–phonon (el–ph) coupling has gained much interest recently. One reason is that the ARPES data in doped metallic cuprates, which showed the broadening of spectral lines at a certain momentum, revealed the band dispersion renormalized by el–ph interaction [11]. In addition, the interaction also shifts the energy of the states.

The doped charge carriers in the presence of both strong electronic correlations and electron–phonon interactions may lead to the formation of a spin–lattice polaron. In particular, the AFM exchange interaction allows for spin flips leading to coherent hole motion at the bottom of the band and forms a spin polaron. In the presence of strong el–ph coupling, both the spin and lattice degrees of freedom become entangled and the spin polaron may transform into a spin–lattice polaron. The formation of this composite polaron may affect both the spin and lattice degrees of freedom locally. Recent ARPES experiments in undoped cuprates were interpreted in terms of strong el–ph coupling giving rise to a localized polaron [12, 13]. The formation of a spin–lattice polaron within the $t-J$ Holstein model has been studied numerically [14–25]. The majority of interest is focused on understanding the interplay between strong electron correlations and the lattice degrees of freedom. The possibility of self-localization of holes in lightly doped cuprates has been discussed [14]. A strong local interplay between antiferromagnetism, polarons and superconducting pairing around a real-space polaron by an impurity has been revealed [15]. It has been found that the effect of el–ph interaction on spin polaron is strongly enhanced as compared to the polaron in uncorrelated systems [16–20, 23].

Recent atomically resolved scanning tunneling microscopy (STM) studies [26–29] on strongly underdoped cuprates revealed a surprisingly local density of states (LDOS) modulation pattern with the square symmetry of the lattice broken on a local scale. The origin of the four-fold symmetry breaking is still controversial [30–34]. Possible scenarios include the emergence of various types of spontaneous translational symmetry breaking states. In one previous study, the origin of this broken local symmetry was attributed to the dopant impurity effect [31]. The broken symmetry states were shown to appear in the case of a hole confined to a cluster of sites centered at an impurity. Meanwhile the introduction of el–ph interaction to the $t-J$ model may stabilize the half-doped stripes [35]. In the presence of strong el–ph coupling, the variations of hopping integral and spin–spin correlation around the impurity may become more remarkable and the composite spin–lattice polaron may appear.

In this paper, we shall discuss the formation of the spin–lattice polaron and its relevance to local symmetry by investigating the Holstein $t-J$-like models with the exact diagonalization method. Due to the interplay of competing electronic correlations and el–ph interactions, the doped hole may either move through the lattice freely or favor the composite spin–lattice polaron. The formation of the Holstein polaron breaks the translational symmetry by suppression of AFM correlations and inducement of FM correlations locally. Moreover, the breaking of local rotational symmetry around the polaron center has been shown. The ground state is generically a parity singlet and the first excited state maybe a parity doublet. Further consequences of the tunneling spectra for comparison with STM experiments will be discussed.

The two-dimensional single-band Holstein t–t'–J model in the adiabatic limit is defined by the Hamiltonian

$$\mathcal{H} = -t \sum_{\langle i,j \rangle \sigma} (c_{i\sigma}^\dagger c_{j\sigma} + \text{h.c.}) - t' \sum_{\langle\langle i,j \rangle\rangle \sigma} (c_{i\sigma}^\dagger c_{j\sigma} + \text{h.c.}) + J \sum_{\langle i,j \rangle} \boldsymbol{S}_i \cdot \boldsymbol{S}_j - g \sum_i u_i n_i^h + \frac{K}{2} \sum_i u_i^2,$$

(1)

where $c_{i,\sigma}^\dagger$ is an electron creation operator with spin σ at site i with a constraint of no double electron occupation due to strong electron correlations, S_i is a spin operator for electron at site i, $\langle i, j \rangle$ and $\langle\langle i, j \rangle\rangle$ refer to NN and NNN sites i and j. The first three terms in equation (1) represent the usual t–t'–J model Hamiltonian. The fourth term denotes the el–ph interaction. In the adiabatic limit, displacements u_i have been treated classically and determined by the minimization of the total energy including electron–electron interaction plus electron–lattice interaction. The hole density operator n_i^h is defined as $n_i^h = 1 - n_i = 1 - \sum_\sigma c_{i,\sigma}^\dagger c_{i,\sigma}$. The last term is lattice elastic energy with elastic force constant K. The energy spectrum and eigenstates can be obtained through exact diagonalization method. The symmetry of the lowest energy state is sensitive to boundary conditions and parameters. In our calculations, we choose $t = K = 1$, suitable for the cuprates, and adopt the periodic boundary condition.

Employed with the exact diagonalization method for a finite 16-site square cluster, the low-lying electronic states have been calculated as a function of el–ph coupling constant g. Due to the competition between electronic correlations and electron–lattice interactions, the ground state has certain limiting cases. When g is very small, the ground state must correspond to a delocalized state, that is to say, a doped hole may move through lattice freely so that the average occupation number of holes at each site is uniform. The presence of a strong el–lattice interaction may clearly favor the localized hole state, which is a sliding periodic polaron lattice. Since we focus on the local properties of polaron, we use a very weak impurity to break the translational symmetry and pin down the sliding polaron lattice so that the doped single hole may stay around a certain site. At $g \gg 1$ limit, the doped hole tends to be localized and results in large lattice distortion around that site. The corresponding ground state is a localized state with polaron formation. The evolution of total energy as well as kinetic energy of the system as a function of g is depicted in figures 1(a) and (b), respectively. The critical el–ph coupling $g_c \sim 1.3$ can be straightforwardly determined by distinguishing these two distinct states. Moreover we use the quantity $\langle d \rangle$ to measure the size of polaron qualitatively, $\langle d \rangle = \sum_i r_i \cdot n_i^h(r_i)$, where r_i is the distance between site i and polaron center. It is obvious that the larger $\langle d \rangle$ value may correspond to a larger polaron size. As shown in the inset of figure 1, as g increases, doped holes tend to concentrate at the polaron center so that the quantity $\langle d \rangle$ may be significantly suppressed. It is worth to mention that the critical point g_c is more clearly revealed in the behaviors of $\langle d \rangle$ and kinetic energy than that of the total energy. Compared with the previous study on the dopant impurity effect [31], the strong variations of hopping integral and spin–spin correlation around the polaron may lead to the formation of local lattice distortion and the appearance of tightly bounded spin–lattice polaron due to strong el–ph coupling [14]. It is worth mentioning that there is no transition to a localized state in the Holstein t–J model and instead it is a crossover to a very heavy spin–lattice polaron with nearly vanishing weight of the quasiparticle if the lattice degrees of freedom are treated fully quantum mechanically. The reason why we study the formation of a polaron in the adiabatic limit is due to the fact that we want to explicitly explore the local symmetry of a localized spin–lattice polaron.
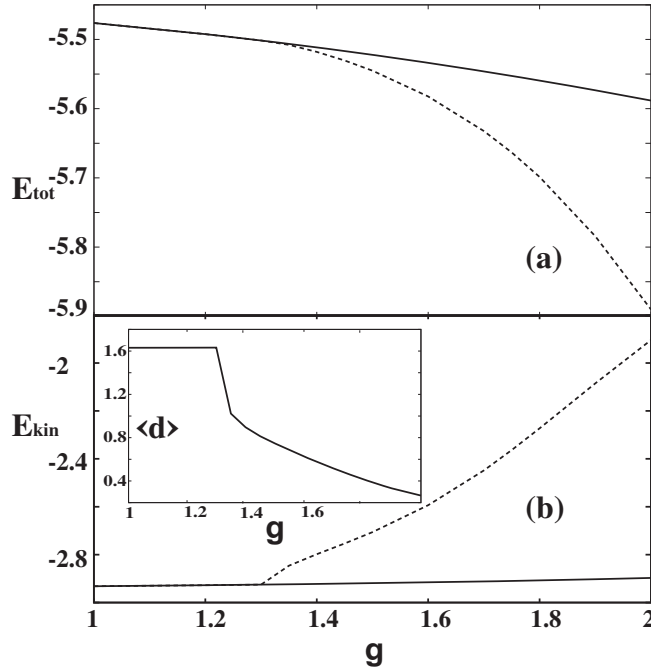
Figure 1. The total energy (a) and kinetic energy (b) as a function of el–ph coupling constant g. The solid line corresponds to the delocalized state while the dashed line denotes the localized Holstein polaron state. The inset shows a measure of polaron size $\langle d \rangle$ as a function of g. We choose $t' = -0.1$ and $J = 0.3$.

Next we examine the effect of NNN hopping integral t'. As we know, the t' term plays an important role in understanding the superconducting correlations in cuprate superconductors [36–38]. In particular, the positive t' case corresponds to the electron-doped system while the negative t' case corresponds to the hole-doped system. In the following, we systematically study the dependence of g_c as a function of t' for two distinct t–J like models. Due to the competing tendency between the polaron formation with strong el–ph interaction and the itinerant electrons with large kinetic energy, we naturally expect that the formation of a localized polaron may require stronger el–ph interaction to compensate for the larger kinetic energy $|t'|$ term. For the Holstein t–t'–J model, it is indeed the case shown in figure 2(a) where g_c increases as $|t'|$ increases. Another feature shown in figure 2(a) is the asymmetrical behavior between $t' < 0$ and $t' > 0$ regions. An intuitive physical understanding of such an effect can be given as follows: for positive t', the t' and t terms in kinetic energy match quite well, so that the positive t' term may enhance the kinetic energy more effectively than the negative t' term, and hence require stronger el–ph interaction g_c to realize the localization of a Holstein polaron. In [24], they found that the quasiparticle is much more coherent and has smaller effective mass in the electron-doped case, which leads to less effective el–ph coupling, and higher g_c is required to enter the small polaron (localized) regime. Their results are consistent with ours.

As suggested in recent studies, the t–t'–J–J' model may be suitable for iron-based superconductors [39, 40]. In such systems, the appropriate range of t' is much larger than that of cuprates and the NNN superexchange coupling is expressed as $J'/J = (t'/t)^2$. In the case of weak t' term, the results are similar to that of the Holstein t–t'–J model. The competing nature between the J' term and the J term may lead to the effect of geometric frustration. In such
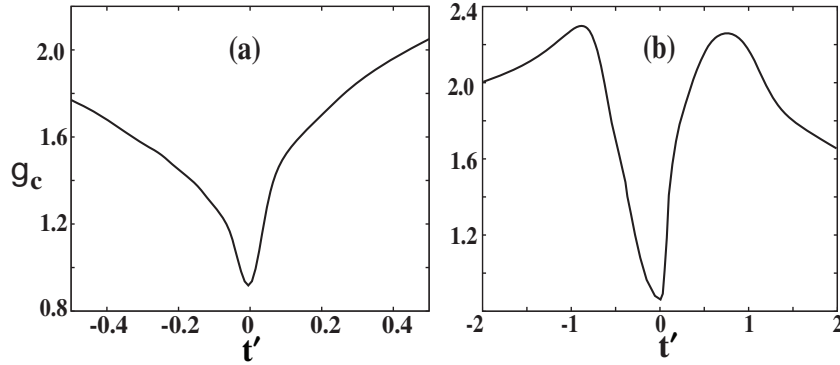
Figure 2. The critical el–ph coupling g_c as a function of t' for Holstein t–t'–J model (a) and t–t'–J–J' model (b). We choose $J = 0.3$ and $J'/J = (t'/t)^2$.

systems, the pairwise J' interaction does not coincide with the square lattice geometry, which may suppress the NN AFM correlation functions. For stronger t' terms as well as J' terms, the suppression may become so strong that the local FM correlation may emerge around the polaron center. And it may result in the enhancement of kinetic energy and the reduction of the critical el–ph interaction g_c, which makes the formation of a polaron easier. These relationships are clearly exhibited in figure 2(b) where g_c decreases as t' becomes quite large.

Similar to the dopant impurity case [31], the presence of a localized spin–lattice polaron may affect not only the local charge and local spin distributions but also the symmetry of the ground state wavefunction. In the following, we adopt the same parity symmetry to characterize different quantum states [31]. In particular, we focus on the reflection symmetries of a two-dimensional square lattice with respect to x- and y-axes passing through the center of the polaron (P_x and P_y respectively) and on the parity $P_x P_y$. Since $[P_{x(y)}, H] = 0$, we may classify states according to the quantum numbers of P_x, P_y. We denote the state with ($P_x = +1$, $P_y = +1$) as state (++), doubly degenerate state $(+1, -1)$, and $(-1, +1)$ as states (+−) and (−+), and $(-1, -1)$ as state (−−). As we know, in the absence of el–ph interactions, for a 16-(4×4) site cluster with periodic boundary condition, the ground state of a single hole in the t–t'–J model has a four-fold symmetry for $t' < 0$, which can be represented by their parity symmetry (++), (+−), (−+), (−−).

As clearly shown in figure 3, the ground states have four-fold degeneracies for weak el–ph interaction $g < g_c \sim 1.3$. When g becomes slightly larger than g_c, such degeneracies are broken. We note that the four low-lying states with different reflection symmetries are quite close in energy. The state with (++) symmetry always has the lowest energy, the doubly degenerated states with parity symmetry (+−) and (−+) correspond to the first excited states, while the state with (−−) symmetry is the second excited state. As g exceeds 1.5, the state (++), originally at much higher energy, may drop down significantly and cross the singly degenerated (−−) state. For $g > 1.7$, both of the two lowest energy states have the (++) symmetry. According to our numerical results, the ground state of spin–lattice polaron is quite robust in the (++) symmetry. We note here that full quantum mechanical description may always lead to the four-fold reflection degeneracy irrespective of the strength of the el–ph coupling [24].

To further explore the interplay between spin and charge degrees of freedom, we study the spatial distribution of the spin–spin correlation function and the hopping integral around the polaron. As depicted in table 1, we show the expectation value of the spin–spin correlation
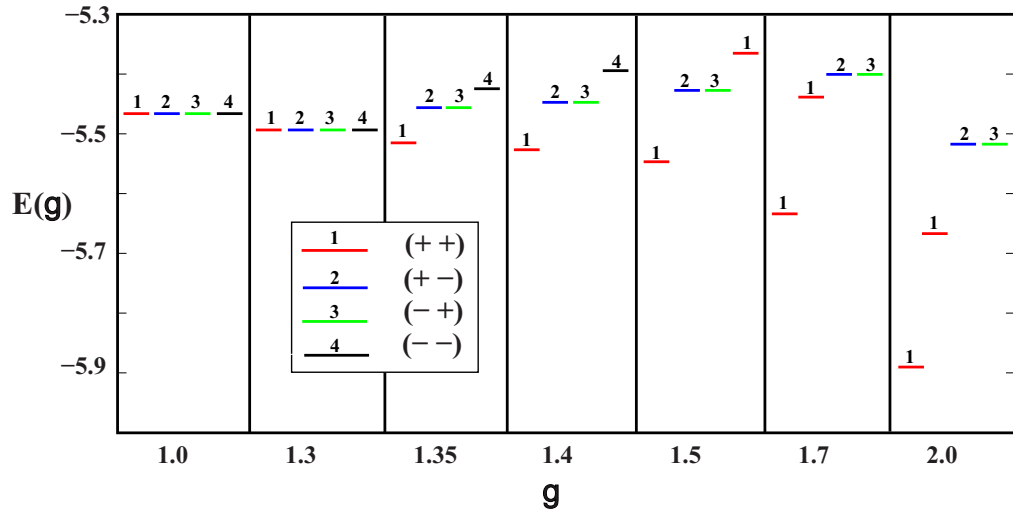
Figure 3. Evolution of four low-lying energy levels and their corresponding parity symmetries as a function of el–ph coupling g. We choose $t' = -0.1$ and $J = 0.3$.

Table 1. The spin–spin correlation functions and hopping integrals for various bonds in a 16-site cluster with periodic boundary condition at $t' = -0.1$, $J = 0.3$ and $g = 2.0$. The bond indices are labeled in figure 4(a).

Bond index	1	2	3	4	5	6
$-\langle \mathbf{S}_i \cdot \mathbf{S}_j \rangle$	−0.034	0.335	0.342	0.337	0.346	0.347
$\langle c_i^\dagger c_j \rangle$	0.405	0.018	0.021	0.002	0.002	0.000

function $\langle S_i S_j \rangle$ as well as the hopping integral $\langle c_i^\dagger c_j \rangle$ for six distinct bonds illustrated in figure 4(a). The interplay of strong correlation and el–ph interaction may lead to hole localization and result in a remarkable hopping integral and a weak FM spin–spin correlation function around the hole. In particular, the AFM correlation along bond 1 is completely suppressed, and a weak FM correlation emerges. The spin–spin correlation function recovers quickly to the value -0.34 for farther bonds. Meanwhile the hopping integral along bond 1 is much stronger than that of the rest bonds and the hopping integral vanishes quickly close to the lattice boundary. It is rather clear that the inducement of local FM correlations around the polaron may help the hole to move around more efficiently, then maximize the local kinetic energy. Hence the mutual cooperative effect between spin and lattice degrees of freedom has been clearly revealed. For the Holstein $t–J$ model in infinite dimensions, the interplay between the formation of a lattice and magnetic polaron in the case of a single hole in the AFM background has been studied before [41]. It shows that the presence of AFM correlations favors the formation of the lattice polaron at lower values of the el–ph coupling. Our numerical calculations agree well with their results.

Furthermore, we investigate the parameter dependence of the spin–spin correlation function for both the $t–t'–J$ model and the $t–t'–J–J'$ model. For these two models, the spin–spin correlation function on bond 1 and bond 2 shows quite different behavior. For the $t–t'–J$ model,

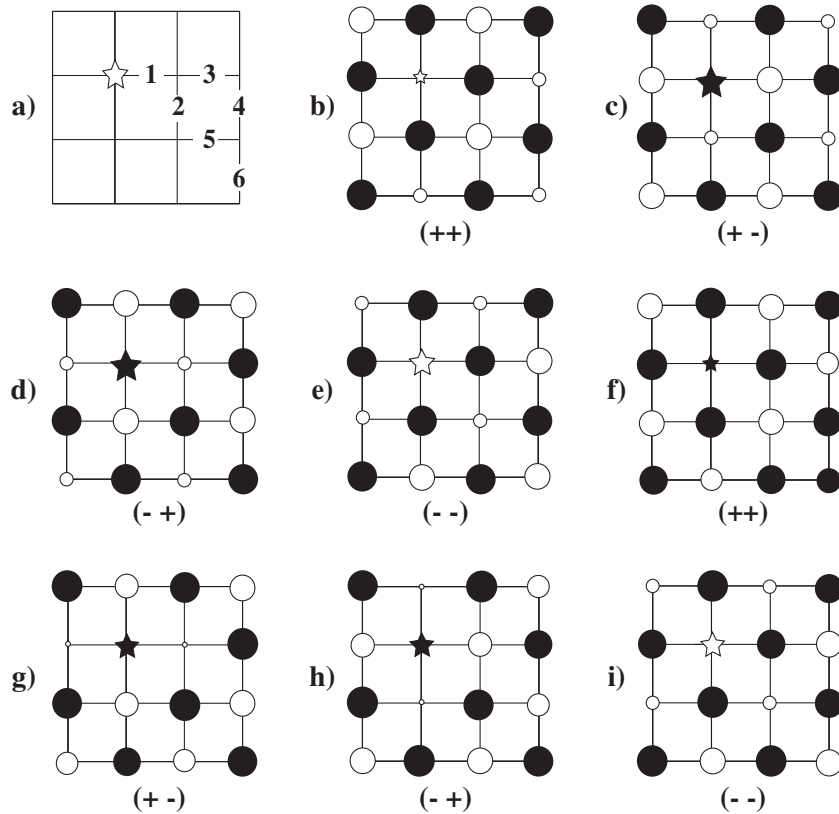**Figure 4.** The spatial distribution of S_z for t–t'–J model. Delocalized states are shown in (b)–(e) for different parity symmetries. Localized states are shown in (f)–(i). The diameter of each circle is proportional to the value of local $|S_z|$. White (black) circle represents up (down) spin. The star symbol labels the center of the polaron.

there is always large AFM correlation on bond 2, while weak AFM or FM correlation shows up on bond 1. This strong suppression of AFM correlation locally around the center of polaron is due to the dramatic lattice distortion or the polaron formation. However, such strong suppression of the AFM correlation on bond 2 may be significantly modified in the t–t'–J–J' model for the large t' case. In such a case, the introduction of large t' may lead to the enhancement of kinetic energy and the strong frustration effect due to the J' term may greatly suppress the AFM correlation on bond 2. Meanwhile, the size of the spin–lattice polaron may be enlarged.

We note here that the suppression of g_c for polaron formation by the stronger AFM correlations is not yet a settled issue. Some studies have found the opposite effect in the Holstein–Hubbard model. In [21, 22], the authors employed AFM dynamical mean field approximation (DMFT) to study the effects of the Coulomb repulsion on the electron–phonon interaction at both half-filling and finite doping cases. In particular, they found the net effect of the Coulomb interaction is a moderate suppression of g_c. The discrepancies may be due to the different models and approximations we used. For instance, the AFM-DMFT is rather accurate for the half-filled Holstein–Hubbard model.

To understand the nature of states with different parity symmetries, the spatial distribution of S_z has been calculated and illustrated in figure 4. For delocalized states, as shown in

figures 4(b)–(e), states with four distinct parity symmetries (++), (+−), (−+), (−−) for the t–t'–J model display quite different patterns. In figure 4(b), for a state with (++) symmetry, weak up spin appears at the polaron center while weak AFM correlation appears between the polaron center and its four nearest neighbors. In figures 4(c) and (d), for states with (+−) and (−+) symmetry, the asymmetry between two neighboring sites of polaron center along x- and y-directions is clearly shown. For localized states, the spatial distribution of S_z patterns are shown in figures 4(f)–(i), respectively, corresponding to different symmetry states. For (++) symmetry state, weak down spin appears at the polaron center while weak FM correlation appears between the polaron center and its four nearest neighbors. As we know, the doped hole may concentrate at the polaron center where the weak FM correlation may emerge. It is obvious that this (++) symmetry state is energetically favorable to the spin–lattice polaron formation. In figures 4(g) and (h), the asymmetry between two neighboring sites of polaron center along x- and y-directions becomes more significant than the delocalized states. Of all four parity symmetry states, this (++) symmetry state has the lowest energy. In addition, we checked the spatial distribution of S_z in the t–t'–J–J' model and similar results are obtained. In both cases, the ground state of spin–lattice polaron prefers the (++) parity symmetry.

In order to check the existence of spin–lattice polaron, integrated differential conductance as a function of cutoff voltage is calculated to be compared with future STM experiments. Following the STM tunneling theory [42], we write the integrated current at **r** up to a positive voltage V as

$$I(\mathbf{r}, \omega) \propto \sum_{\sigma, m} |\langle m | a_{\mathbf{r}, \sigma}^{\dagger} | \psi^{1h} \rangle|^2 \theta(\omega - E_m + E^{1h}), \tag{2}$$

where $a_{\mathbf{r}, \sigma}^{\dagger}$ is the electron creation operator with spin σ at site **r**, $|m\rangle$ are eigenstates of the half-filled system with energy E_m, $\omega = \text{eV}$, and θ is a step function. The $|\psi^{1h}\rangle$ denotes the single-hole eigenstate with energy E^{1h}. In the following, we show the I–ω curve on various sites and for different el–ph coupling g. For convenience, we shift the origin of x-axis by $\omega_0 = \omega + \omega_{\text{ex}}$ where $\omega_{\text{ex}} = E_0 - E_0^{1h}$ and E_0, E_0^{1h} correspond to the ground state of half-filled system and single-hole system, respectively. Here we consider the contributions from low-lying energy states of the single-hole system.

As we know already, the doped hole tends to stay around the polaron center and the hole density at the polaron center is more significant than that on other sites by increasing the el–ph interaction g. Thus we expect the integrated current at the polaron center to become larger when g increases. This result is clearly shown in the left panel of figure 5. In the case of impurity doped cuprates, the conductance pattern is anisotropic as the tip of a tunneling microscope scans above the Cu–O–Cu bonds along the $x(y)$-axes. This anisotropy is quite pronounced at voltage around $\omega \sim J$. In the present case, due to the formation of spin–lattice polaron, the ground state of the one-hole system has (++) symmetry, the first excited state corresponds to the doubly degenerated states (+−) and (−+). The presence of quadrupole interaction of two single-hole states or by other couplings may not change the symmetry of the ground state but may destroy the two-fold degeneracy of the first excited state. We consider the system to be in one of the two degenerate states, say in the state of (+−). As depicted in the right panel of figure 5, below certain cutoff-energy ($\sim 0.11\,J$), the integrated current shows four-fold rotational symmetry for the state with (++) symmetry. For the higher cutoff-energy, the first excited state with (+−) symmetry may play an important role in the local symmetry breaking for the signals along x and y-directions.
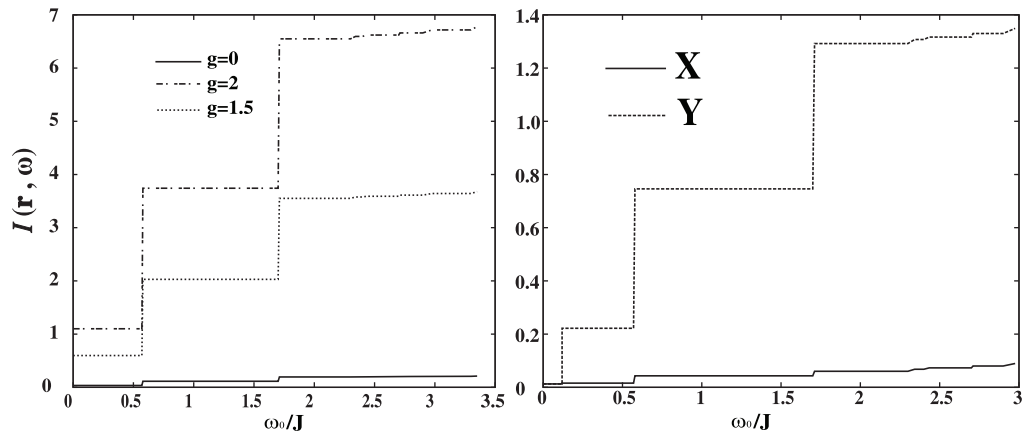
Figure 5. The local integrated current up to voltage V for different sites at various el–ph coupling constant g as a function of ω. The left panel shows the results for signal at the center of polaron for different g values. The right panel depicts the results for signals at the two NN sites respectively along the x- and y-directions at $g = 2.0$.

In [27, 29], a sequence of identical experiments were carried out on two different cuprates at the same strongly underdoped $Ca_{1.88}Na_{0.12}CuO_2Cl_2$ and $Bi_2Sr_2Dy_{0.2}Ca_{0.8}Cu_2O_{8+\delta}$, the virtually identical local rotational symmetry breaking phenomena were observed. The authors believed that these identical phenomena must occur due to the common characteristic of these two quite different materials. In the present study, we attribute the rotational symmetry breaking in the LDOS of the cuprates to the formation of localized spin–lattice polaron which is also a common characteristic of very underdoped system with both strong electronic correlations as well as strong el–ph interactions. However, the origin of the local symmetry breaking is still controversial. Possible scenarios include the emergence of various types of spontaneous translational symmetry breaking states. A fluctuating Cu–Cu bond model was proposed which takes into account the nonlinear modulation of the Cu–Cu bond by planar oxygen vibrations [32]. The dominant fluctuations are manifested in a pattern of oxygen vibrational square amplitudes with quadrupolar symmetry around a given Cu site. The formation of a static d-wave charge density wave state may reduce C_4 symmetry to C_2 within each four-Cu-atom plaquette. There are some other theoretical proposals such as a nematic electronic liquid crystal of nanodomains [30], a hypothesis of pair-density wave state or striped superconducting state [33], and the coexistence of valence bond order with nodal quasiparticles [34].

In the broken rotational symmetry state observed in the STM data, the local charge density at each of the four NN Cu sites is almost uniform but the asymmetry is most pronounced at the in-plane oxygen sites. However, some scenarios based on charge orders may give rise to the asymmetry of local charge density at each of four NN Cu sites. In our present polaron scenario, the local charge density around the localized Holstein polaron still obeys the four-fold rotational symmetry while the conductance pattern of the broken symmetry state is anisotropic as the tip of a tunneling microscope scans above the Cu–O–Cu bonds along the $x(y)$-axes. Our polaron scenario agrees qualitatively with recent data from STM showing broken local rotational symmetry.

Our numerical results can be qualitatively understood in terms of the renormalized mean-field method for the $t-J$ model. Due to the presence of a spatial inhomogeneous polaron, the

renormalized factor g_t and g_s become site-dependent. According to a previous study [43], the renormalized factor of kinetic energy on the bond connecting two sites i and j can be expressed as $g_t^{ij} \sim \sqrt{\delta_i \delta_j}$. As we know, in the case of strong el–ph interaction, the hole density is highly localized at the center of Holstein polaron. It is obvious that the bonds with appreciable hopping integral only appear around the polaron and may result in the suppression of the AFM correlation locally. For the delocalized states, g_t^{ij} is simply a constant, as is the AFM correlation function. The above qualitative analysis agrees reasonably well with our numerical results shown in figure 3 and table 1.

In summary, we study both the formation and local symmetry of spin–lattice polaron semiclassically in the planar Holstein $t–J$-like models within the exact diagonalization method. Due to the interplay of competing interactions among electronic correlations and el–ph interactions, the doped hole may either move freely or lead to the localized spin–lattice distortion and form a Holstein polaron. Since the formation of polaron breaks the translational symmetry, we use the parity symmetry with respect to the polaron center to characterize the localized states. The presence of spin–lattice polaron may suppress the AFM correlations and induce the FM correlations locally around the polaron. This effect may further stabilize the spin–lattice polaron. Moreover, this effect may lead to a strong localized state with (++) parity symmetry as ground state. Moreover, the breaking of local rotational symmetry around the polaron has been shown for certain voltage cutoff. The present investigation on the polaron formation and local symmetry may provide useful information for understanding STM experimental observations.

Acknowledgments

References

[1] Lee P A, Nagaosa N and Wen X G 2006 *Rev. Mod. Phys.* **78** 17
[2] Nagaoka Y 1966 *Phys. Rev.* **147** 392
[3] Dagotto E, Moreo A and Barnes T 1989 *Phys. Rev.* B **40** 6721
[4] Dagotto E 1994 *Rev. Mod. Phys.* **66** 763
[5] White S R and Affleck I 2001 *Phys. Rev.* B **64** 024411
[6] Lee T K, Ho C M and Nagaosa N 2003 *Phys. Rev. Lett.* **90** 067001
[7] Röder H, Fehske H and Buttner H 1993 *Phys. Rev.* B **47** 12420
[8] Danmascelli A, Shen Z-X and Hussain Z 2003 *Rev. Mod. Phys.* **75** 473
[9] Kim C, White P J, Shen Z-X, Tohyama T, Shibata Y, Maekawa S, Wells B O, Kim Y J, Birgeneau R J and Kastner M A 1998 *Phys. Rev. Lett.* **80** 4245
[10] Tohyama T and Maekawa S 2000 *Supercond. Sci. Technol.* **13** R17
[11] Lanzara A *et al* 2001 *Nature* **412** 510
[12] Shen K M *et al* 2004 *Phys. Rev. Lett.* **93** 267002
[13] Shen K M *et al* 2007 *Phys. Rev.* B **75** 075115

IOP Institute of Physics Φ DEUTSCHE PHYSIKALISCHE GESELLSCHAFT

[14] Prelovšek P, Zeyher R and Horsch P 2006 *Phys. Rev. Lett.* **96** 086402

[15] Johnston S, Vernay F and Devereaux T P 2009 *Europhys. Lett.* **86** 37007

[16] Mishchenko A S and Nagaosa N 2004 *Phys. Rev. Lett.* **93** 036402

[17] Rösch O, Gunnarsson O, Zhou X J, Yoshida T, Sasagawa T, Fujimori A, Hussain Z, Shen Z-X and Uchida S 2005 *Phys. Rev. Lett.* **95** 227002

[18] De Filippis G, Cataudella V, Mishchenko A S and Nagaosa N 2007 *Phys. Rev. Lett.* **99** 146405

[19] Zhong J and Schüttler H B 1992 *Phys. Rev. Lett.* **69** 1600

[20] Röder H, Fehske H and Büttner H 1993 *Phys. Rev.* B **47** 12420
Fehske H, Röder H, Wellein G and Mistriotis A 1995 *Phys. Rev.* B **51** 16582
Bäuml B, Wellein G and Fehske H 1998 *Phys. Rev.* B **58** 3663

[21] Sangiovanni G, Capone M, Castellani C and Grilli M 2005 *Phys. Rev. Lett.* **94** 026401

[22] Sangiovanni G, Gunnarsson O, Koch E, Castellani C and Capone M 2006 *Phys. Rev. Lett.* **97** 046404

[23] Gunnarsson O and Rösch O 2006 *Phys. Rev.* B **73** 174521

[24] Bonca J, Maekawa S, Tohyama T and Prelovsek P 2008 *Phys. Rev.* B **77** 054519

[25] Vidmar L and Bonca J 2010 *Phys. Rev.* B **82** 125121

[26] Hanaguri T, Lupien C, Kohsaka Y, Lee D-H, Azuma M, Takano M, Takagi H and Davis J C 2004 *Nature* **430** 1001

[27] Kohsaka Y *et al* 2007 *Science* **315** 1380

[28] Kohsaka Y *et al* 2008 *Nature* **454** 1072

[29] Schmidt A R, Fujita K, Kim E-A, Lawler M J, Eisaki H, Uchida S, Lee D-H and Davis J C 2011 *New J. Phys.* **13** 065014

[30] Kivelson S A, Fradkin E and Emery V J 1998 *Nature* **393** 550

[31] Chen Y, Rice T M and Zhang F C 2006 *Phys. Rev. Lett.* **97** 237004

[32] Newns D M and Tsuei C C 2007 *Nature Phys.* **3** 184

[33] Berg E, Fradkin E and Kivelson S A 2009 *Phys. Rev.* B **79** 064515

[34] Vojta M and Rösch O 2008 *Phys. Rev.* B **77** 094504

[35] Chou C-P and Lee T K 2010 *Phys. Rev.* B **81** 060503
Chou C-P and Lee T K 2012 *Phys. Rev.* B **85** 104511

[36] Pavarini E, Dasgupta I, Saha-Dasgupta T, Jepsen O and Andersen O K 2001 *Phys. Rev. Lett.* **87** 047003

[37] Lee W C, Lee T K, Ho C M and Leung P W 2003 *Phys. Rev. Lett.* **91** 057001

[38] Shih C T, Lee T K, Eder R, Mou C-Y and Chen Y C 2004 *Phys. Rev. Lett.* **92** 227002

[39] Si Q and Abrahams E 2008 *Phys. Rev. Lett.* **101** 076401

[40] Fang C, Yao H, Tsai W F, Hu J P and Kivelson S A 2008 *Phys. Rev.* B **77** 224509

[41] Cappelluti E and Ciuchi S 2002 *Phys. Rev.* B **66** 165102

[42] Tersoff J and Hamann D R 1985 *Phys. Rev.* B **31** 805

[43] Wang Q H, Wang Z D, Chen Y and Zhang F C 2006 *Phys. Rev.* B **73** 092507